ACS Medicinal Chemistry Letters

pubs.acs.org/acsmedchemlett Letter

Antiferroptotic Activity of Phenothiazine Analogues: A Novel Therapeutic Strategy for Oxidative Stress Related Disease

Jun Liu, Indrajit Bandyopadhyay, Lei Zheng, Omar M. Khdour,* and Sidney M. Hecht*

Cite This: https://dx.doi.org/10.1021/acsmedchemlett.0c00293 Read Online

ACCESS | Metrics & More | Article Recommendations | Supporting Information

ABSTRACT: Ferroptosis is an iron-catalyzed, nonapoptotic form of regulated necrosis that has been implicated in the pathological cell death associated with various disorders including neurodegenerative diseases (e.g., Friedreich's ataxia (FRDA), Alzheimer's disease, and Parkinson's disease), stroke, and traumatic brain injury. Recently, we showed that lipophilic methylene blue (MB) and methylene violet (MV) analogues both promoted increased frataxin levels and mitochondrial biogenesis, in addition to their antioxidant activity in cultured FRDA cells. Presently, we report the synthesis of series of lipophilic phenothiazine analogues that potently inhibit ferroptosis. The most promising compounds (**1b**−**5b**) exhibited an improved protection compared to the parent phenothiazine against erastin- and RSL3-induced ferroptotic cell death. These analogues have equivalent or better potency than ferrostatin-1 (Fer-1) and liproxstatin-1 (Lip-1), that are among the most potent inhibitors of this regulated cell death described so far. They represent novel lead compounds with therapeutic potential in relevant ferroptosis-driven disease models such as FRDA.

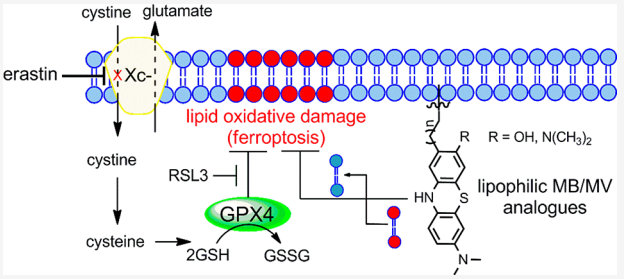

KEYWORDS: *Ferroptosis, Friedreich's ataxia, lipid peroxidation, antiferroptotic activity, methylene blue, methylene violet*

Friedreich's ataxia (FRDA) is a hereditary neurodegenerative disease caused by an intronic GAA repeat in the *FXN* gene that reduces frataxin (FXN) expression.[1,2] Insufficient frataxin impedes iron-containing mitochondrial complex assembly, and the excess iron overloads the mitochondrial matrix,[3−7] triggering the formation of reactive oxygen species (ROS) that contribute to cellular oxidative stress and lipid peroxidation.[8−12] These cellular and molecular features of FRDA are also hallmark features of ferroptosis, a cell death pathway.

Ferroptosis, originally described as a new form of cell death,[13] is an iron-dependent and ROS-dependent form of cell death accompanied by rapid loss of plasma and mitochondrial membrane integrity and prominent changes in mitochondrial morphology.[14−17] These abnormalities result from intense membrane lipid peroxidation and oxidative stress, although the precise mechanism(s) of ferroptotic cell death remains undefined. Cells have evolved systems to block ferroptotic cell death. One central regulators is glutathione peroxidase 4 (GPX4), that together with glutathione (GSH) and other antioxidant defenses prevents lipid peroxidation and ferroptosis (Figure 1).[17−20] Pathways linked to ferroptosis inhibition all converge into GPX4/glutathione (Figure 1).[17−20] RAS-selective lethal 3 (RSL3), a ferroptosis inducer, acts directly on GPX4 and inhibits its activity, leading to ferroptosis.[13,21] GPX4 requires glutathione to reduce lipid hydroperoxides,[22] while GSH synthesis is dependent on cysteine, produced from cystine that itself is imported via the cystine/glutamate antiporter system x_c^- (Figure 1).[23] Erastin (eradicator of RAS and ST-expressing cells) inhibits the cystine/glutamate transporter system x_c^-, leading to cysteine starvation, GSH depletion, and ferroptosis.[13,24] Additionally, a ferroptosis-glutathione-independent pathway was recently identified for suppressing ferroptosis.[25,26] Ferroptosis-suppressor-protein 1 (FSP1), was first shown to counteract ferroptosis in the absence of GPX4.[25,26] FSP1 is an oxidoreductase, reducing ubiquinone (coenzyme Q_{10}) to radical scavenger ubiquinol, thereby limiting lipid peroxidation within membranes, independent of GPX4 or glutathione (Figure 1).[26]

Ferroptosis is believed to be involved in a number of mitochondrial and neurodegenerative diseases.[10,27] Evidence from transgenic FRDA mice-derived neurons, for example, describes a functional imbalance between respiratory chain complexes I and II, driving free radical formation, thereby resulting in glutathione depletion and lipid peroxidation that contribute to neuronal death.[11,12] Recently, reduction of lipid hydroperoxides in fibroblasts and neurons from different FRDA mouse models has also improved FRDA phenotypes and diminished ferroptotic cell death.[10−12] This suggests that targeting ferroptosis pharmacologically, in addition to increas-

Received: May 29, 2020
Accepted: September 15, 2020
Published: September 15, 2020

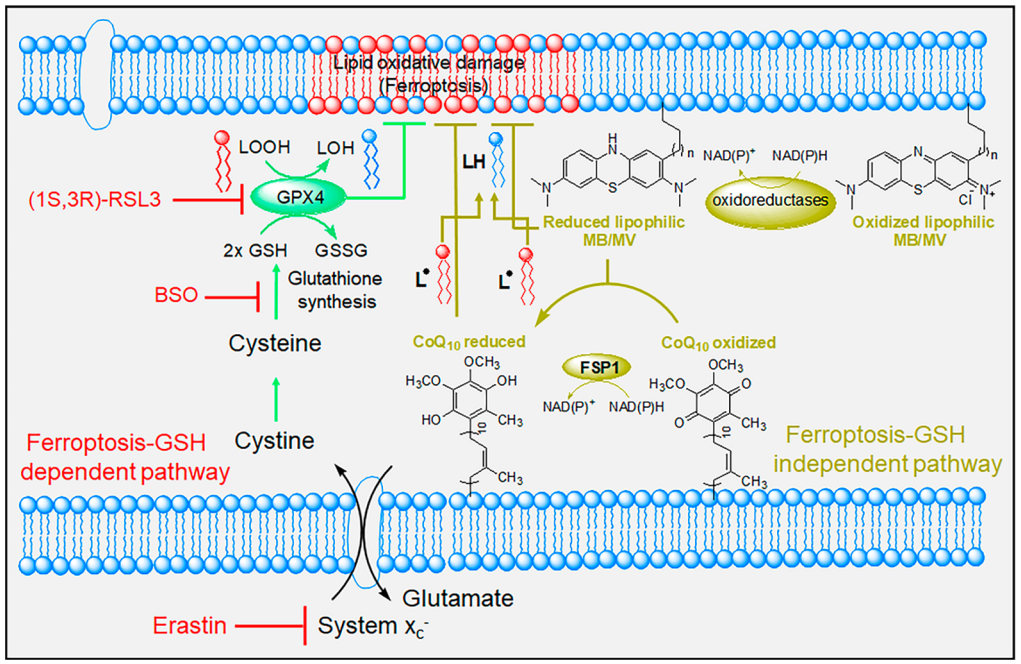

Figure 1. Schematic representation depicting the antiferroptotic function of both GSH-dependent and GSH-independent (FSP1) pathways and the key targeting points. Lipid peroxidation is a hallmark of ferroptosis that is triggered by inhibition of the glutamate-cystine antiporter system (system x_c^-) with erastin or inhibition of GPX4 with RSL3.

ing both FXN and ATP levels, might constitute a beneficial FRDA therapy.

Phenothiazine has a tricyclic aromatic ring containing sulfur and nitrogen atoms and has gained importance for pharmaceutical applications in part due to its redox properties.[28] MB undergoes reversible two-electron oxidation processes at low potential, enabling MB to donate electrons to the electron transport chain in the absence of oxygen, thereby enhancing ATP production and cytochrome *c* oxidase activity and contributing to cell survival via bypassing complexes I−III to generate ATP.[29−32] Recently, we have reported lipophilic phenothiazines that promote increased frataxin levels and mitochondrial biogenesis in cells from FRDA patients with reduced toxicity and better overall activity than MB/MV.[33,34]

Improved ferroptosis inhibitors are thus of great interest. As ferroptosis is accompanied by a burst in lipid peroxidation within plasma and mitochondrial membranes,[35] we hypothesized that lipophilic MB/MV derivatives might be more effective inhibitors of this cell death pathway. A series of lipophilic phenothiazines were synthesized to probe their activity. The prepared analogues were evaluated as *in vitro* inhibitors of ferroptosis, and some exhibited strong antiferroptosis activity, at least comparable to ferroptosis inhibitors such as ferrostatin-1 (Fer-1) and liproxstatin-1 (Lip-1).

We have reported the importance of side chain length for facilitating their effects on the mitochondrial respiratory chain to achieve improved antioxidant activity.[36] Accordingly, we prepared analogues having different side chain lengths attached to the phenothiazine redox core. The syntheses of lipophilic MB analogues **1a−5a**, having alkyl substituents on phenothiazine redox core position 2 (Figure 2), were carried out as described (Scheme 1), employing a Wittig reaction as the key step.[33,34] The MV analogues (**1b−5b**) (Figure 2) were obtained by basic hydrolysis of the corresponding MB analogues **1a−5a** (Scheme 1).[33,34] The antiferroptotic activity of the newly prepared lipophilic phenothiazine analogues **1−5** was tested in selected biochemical and biological assays. Since lipid peroxidation is a hallmark of ferroptotic cell death, we established a lipid peroxidation assay in FRDA patient-derived lymphocyte cells using the GPX4 inhibitor RSL3. After establishing dose-dependent sensitivity to RSL3-mediated ferroptosis, the ability of analogues **1−5** to quench lipid peroxidation was studied in FRDA lymphocytes that had been treated with GPX4 inhibitor RSL3. The fluorescent lipid peroxidation-sensitive fatty acid-conjugated dye (C_{11}-BODIPY$^{581/591}$) probe was used as described.[37] Initially, ferroptosis sensitive FRDA cells were treated with varying concentrations of analogues **1−5** or the validated ferroptosis inhibitors ferrostatin-1 (Fer-1) and liproxstatin-1 (Lip-1) and then with a lethal dose of RSL3 (2 μM). Table 1 shows the activity and potency of tested MB/MV analogues in blocking RSL3-induced lipid peroxidation in FRDA lymphocytes, with low nanomolar EC_{50} values. As summarized in Table 1, both MB and MV analogues were more effective in quenching lipid peroxidation when compared to their parent compounds. Plausibly this might be due to the influence of their side chains on their subcellular localization or mitochondrial membrane lipid rich environment. Interestingly, the redox core also influenced their potency. The MV redox core exhibited better potency than MB when tested at lower concentrations, whereas radical-trapping antioxidants inhibit autoxidation by donating an H atom to the peroxyl radical to give a nonpropagating radical from both the phenolic O−H and aminic N−H of the MV redox core. In this assay the optimal side chain length for MB analogues was 10-carbon atoms, while for MV analogues it was 8−12 carbon atoms (Table 1). MV analogues **1b−5b** have equivalent or better potency than the most potent inhibitors of ferroptosis described so far, notably ferrostatin-1 (Fer-1) and liproxstatin-1 (Lip-1), and are superior to α-TOH (Table 1). Elevated lipid peroxyl radical levels are associated with ferroptosis onset, and many of

https://dx.doi.org/10.1021/acsmedchemlett.0c00293
ACS Med. Chem. Lett. XXXX, XXX, XXX−XXX

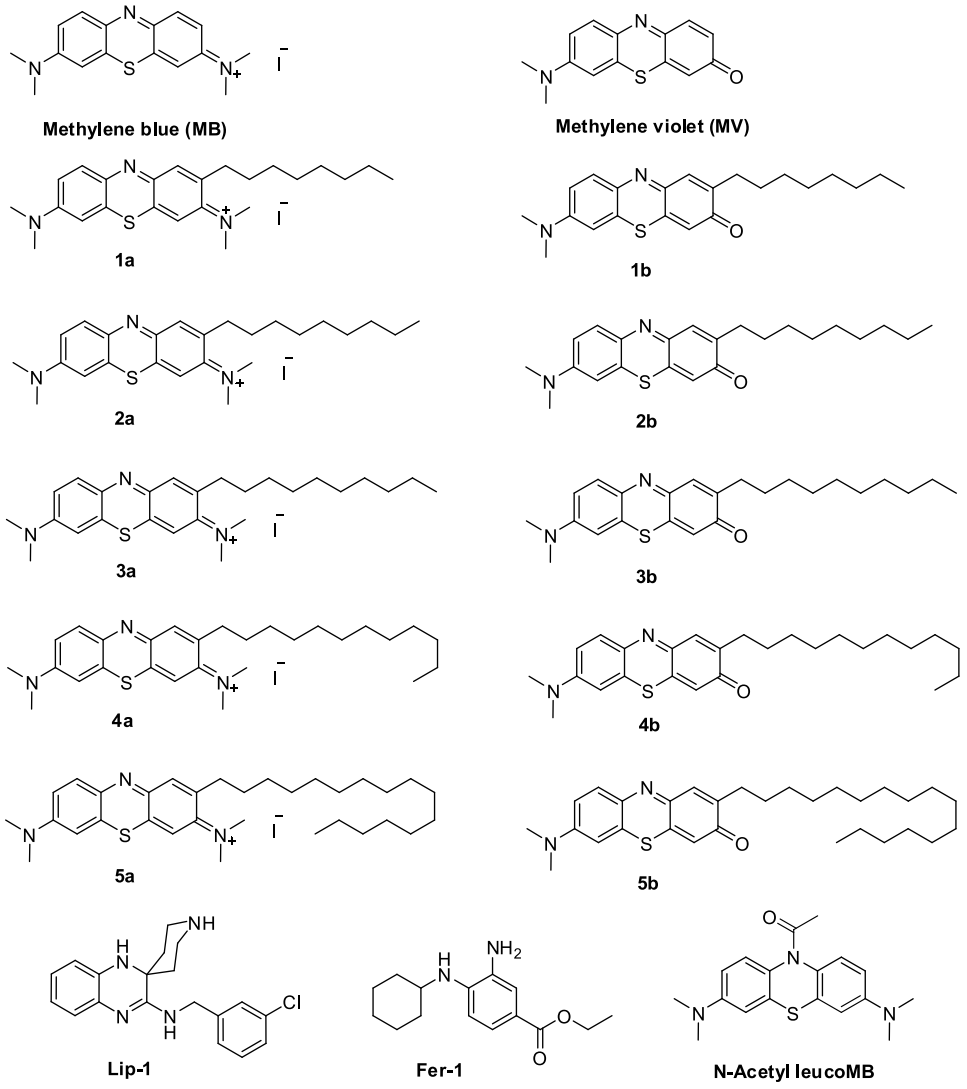

Figure 2. Chemical structures of the synthesized methylene blue (MB) and methylene violet (MV) analogues (**1**−**5**).

the most potent antiferroptotic agents exhibit scavenging of lipid peroxyl radicals. To study the relevance of this mechanism to MB and its derivatives, we modified MB by *N*-acetylation. MB acetylation blocked its redox activity and completely eliminated its antiferroptotic effects (Table 1). To complement the model of lethal RSL3-induced lipid peroxidation by inhibition of GPX4, we employed a second method of inducing ferroptosis that models the GSH depletion and oxidative stress observed in mitochondrial disease patients. Erastin is a classical inducer of ferroptosis; it acts by inhibition of cystine-glutamate exchange at the plasma membrane and as a consequence depletes the cell of GSH (Figure 1).[13,24] We investigated the effects of **1**−**5** on erastin-induced cell death in primary FRDA patient-derived fibroblasts. Erastin-induced cell death was determined by assessing the depletion of cellular ATP using a commercially available luciferase-linked ATPase enzymatic assay (ViaLight Plus proliferation/cytotoxicity Kit, Lonza, Walkersville, MD). As summarized in Table 2, MB/MV analogues potently protected FRDA cells with a trend similar to that noted for RSL3-induced lipid peroxidation in FRDA lymphocytes. Compounds **1b**−**4b** were the most efficient, having EC_{50} values of 15 ± 2, 11 ± 1, 10 ± 1, and 15 ± 1 nM, respectively (Table 2). Again, in this assay the lipophilic analogues were more effective than their redox core parents (MB/MV). The optimal side chain length for MB analogues was 10 carbon atoms (**3a**) and was 8−12 carbon atoms for MV analogues. Compounds having a side chain with 16 carbon atoms (**5a** and **5b**) were less protective. These encouraging findings demonstrated that the MV analogues had better overall antiferroptotic activity than that of MB analogues as well as the well-known ferroptosis inhibitors ferrostatin-1 and liproxstatin-1.

Methylene blue is a recyclable redox core that can donate electrons to cytochrome *c* in the mitochondrial electron transport chain, contributing to increased ATP, as described previously.[29,30,33,38] Frataxin deficiency in FRDA leads to decreased ATP production. Given the hormetic pharmacological effect of MB, exhibiting opposite effects at high and low doses,[39] we used MB in a concentration range (100 nM−2.5 μM) relevant in cellular studies, in particular to those reporting neuroprotective effects of MB.[29−34] Accordingly, MB/MV analogues **1**−**5** were evaluated for their ability to support ATP production in FRDA lymphocytes (Figure 3). Total cellular ATP was measured in a cultured FRDA cell line as described previously.[33,34] The cells were grown on glucose-free media supplemented with galactose. Since cells grown in galactose

https://dx.doi.org/10.1021/acsmedchemlett.0c00293
ACS Med. Chem. Lett. XXXX, XXX, XXX−XXX

Scheme 1. Synthesis of Phenothiazine Analogues

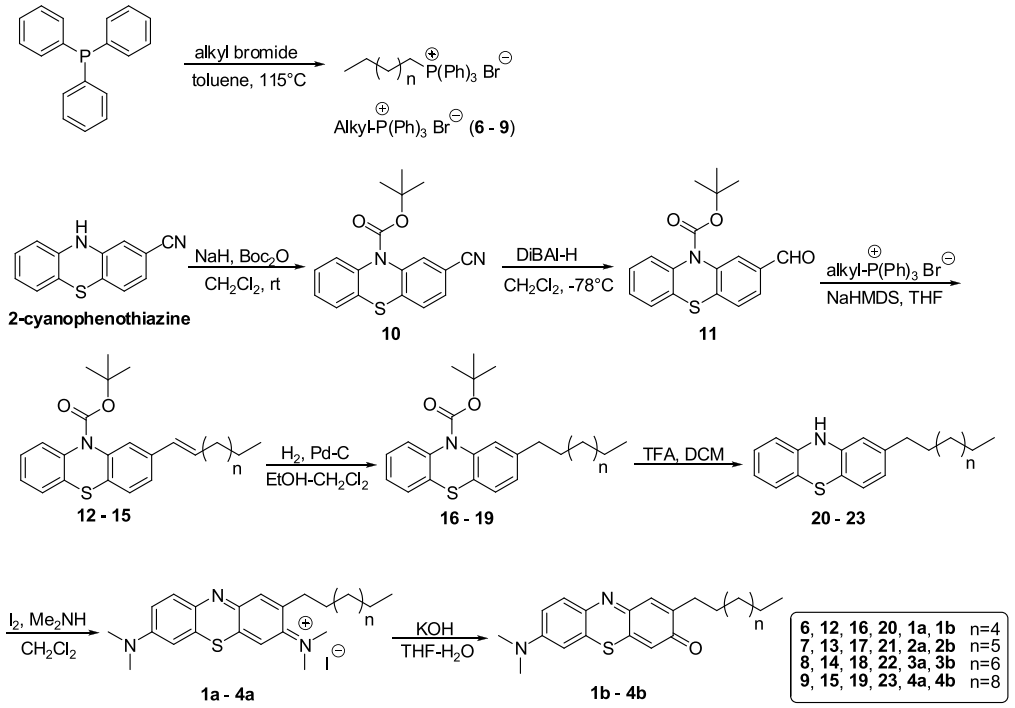

Table 1. Antiferroptotic Effects of MB/MV Analogues (1−5) in FRDA Lymphocytes against RSL3-Induced Lipid Peroxidation[a]

Compound	RSL3 challenge lipid peroxidation inhibition EC_{50} (nM)
MB	88 ± 13
Acetylated MB[b]	>2500
MV	26 ± 3
1a	76 ± 6
1b	14 ± 1
2a	53 ± 3
2b	12 ± 1
3a	38 ± 3
3b	9 ± 1
4a	54 ± 5
4b	16 ± 1
5a	70 ± 5
5b	25 ± 3
Lip-1	22 ± 2
Fer-1	48 ± 2
α-TOH	>500

[a]The calculated EC_{50} values were determined graphically from the dose−response curves using the nonlinear regression curve fit analysis model. [b]*N*-acetyl leucomethylene blue (Figure 2).

Table 2. Effect of MB/MV Analogues (1−5) on the Cellular Viability of Primary FRDA Fibroblasts against Erastin-Induced Ferroptotic Cell Death[a]

Compound	Erastin challenge cell survival EC_{50} (nM)
MB	43 ± 3
MV	27 ± 3
1a	39 ± 3
1b	15 ± 2
2a	37 ± 3
2b	11 ± 1
3a	29 ± 3
3b	10 ± 1
4a	35 ± 1
4b	15 ± 1
5a	55 ± 6
5b	22 ± 2
Lip-1	22 ± 4
Fer-1	33 ± 4
α-TOH	>500

[a]The calculated EC_{50} values were determined graphically from the dose−response curves using the nonlinear regression curve fit analysis model.

rely mostly on oxidative phosphorylation (OXPHOS) to produce their ATP, they become more sensitive to mitochondrial respiratory chain inhibitors than cells grown in normal (glucose) medium. As shown in Figure 3, MB strongly diminished ATP levels in a concentration dependent fashion (0.25, 0.5, and 2.5 μM) in Friedreich's ataxia lymphocytes. MB increased ATP levels slightly when used at 0.1 μM concentration. In contrast, MV itself was less detrimental in inhibiting ATP levels at higher concentrations. Similar results to MB itself were observed for MB analogues, having a short to medium length alkyl substituent chain (8−10 carbon atoms) (**1a**−**3a**). Our earlier study[34] suggested that compounds having lipophilic side chains of 16-carbon atoms (**5a**) exhibit lesser inhibition of mitochondrial respiratory chain complexes and correspondingly permit more effective maintenance of cellular ATP levels. Compound **5a** clearly increased the ATP level when employed at 0.1 and 0.25 μM concentrations, although it suppressed ATP levels when used at 2.5 μM concentration. On the other hand, MV analogues (**1b**−**5b**) with similar substitution patterns of the lipophilic alkyl side chain were also studied in this assay. The MV analogues having a medium length alkyl side chain (8−10 carbon atoms, **1b**−**3b**) increased the ATP level when employed at 0.1 μM concentration but suppressed the ATP level when used at

https://dx.doi.org/10.1021/acsmedchemlett.0c00293
ACS Med. Chem. Lett. XXXX, XXX, XXX−XXX

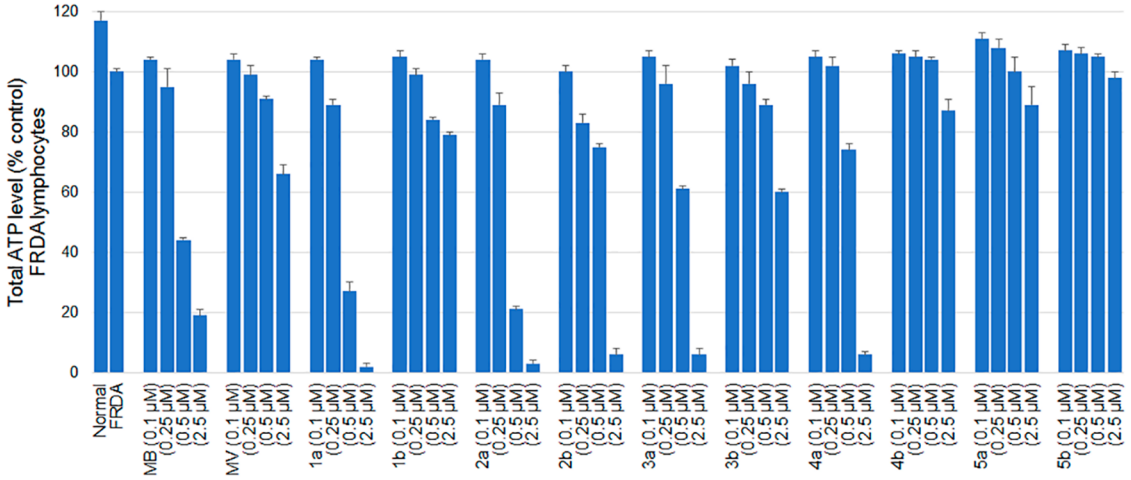

Figure 3. Total ATP levels in FRDA lymphocytes following incubation with test compounds for 24 h in glucose free media (25 mM galactose) to force the cell to employ OXPHOS. Results are expressed as percentage of total ATP relative to untreated control.

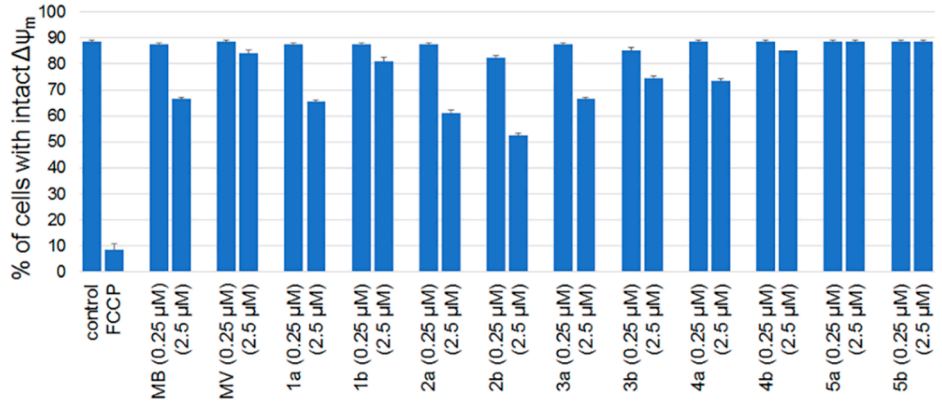

Figure 4. Effects of **1**−**5** on $\Delta\psi_m$ in FRDA lymphocytes using the ratiometric fluorescent marker JC-1. Flow cytometric determination of depolarized $\Delta\psi_m$ using the ratiometric fluorescent probe JC-1. The actual percentage of cells with intact $\Delta\psi_m$ were extracted from a two-dimensional color density dot blot. Results obtained were verified by running duplicates in two independent runs.

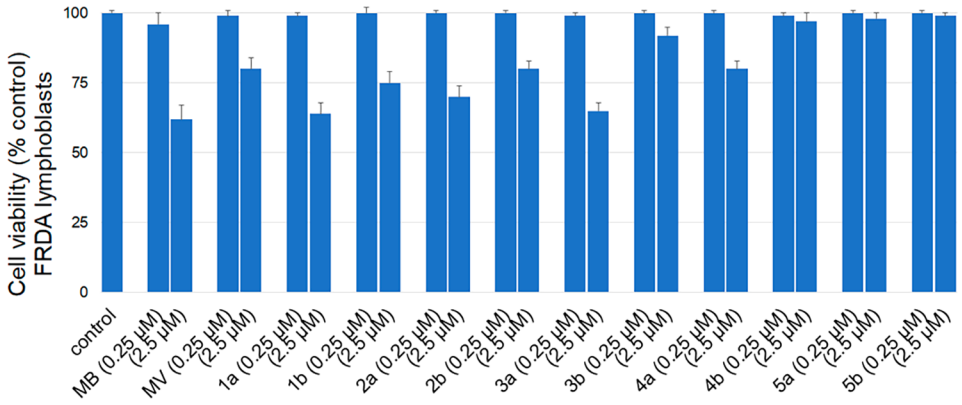

Figure 5. Cytotoxicity of phenothiazine analogues **1**−**5** toward cultured FRDA lymphocytes after incubation for 24 h in glucose-free (galactose) media to force the cells to rely on mitochondrial ATP production. Flow cytometric determination of cell viability by dual fluorescence labeling employed calcein-AM and ethidium homodimer-1 as live and dead stains, respectively. The actual percentage of live cells was extracted from a two-dimensional color density dot blot. Results obtained were verified by running duplicates in two independent experiments.

higher concentrations. The MV analogue with a 12-carbon atom alkyl side chain (**4b**) clearly increased the ATP level when employed at 0.1, 0.25, and 0.5 μM concentrations but suppressed the ATP level slightly when used at 2.5 μM concentration. Compound **5b**, having a 16-carbon atom alkyl side chain, clearly increased the ATP level when employed at 0.1, 0.25, and 0.5 μM concentrations but had little effect on ATP when employed at 2.5 μM concentration. While the concentrations of the MB/MV analogues that had an effect on ATP production are significantly higher than the concentrations of these compounds that block ferroptosis and are thus not likely to be pertinent to the antiferroptotic mechanism(s),

https://dx.doi.org/10.1021/acsmedchemlett.0c00293
ACS Med. Chem. Lett. XXXX, XXX, XXX−XXX

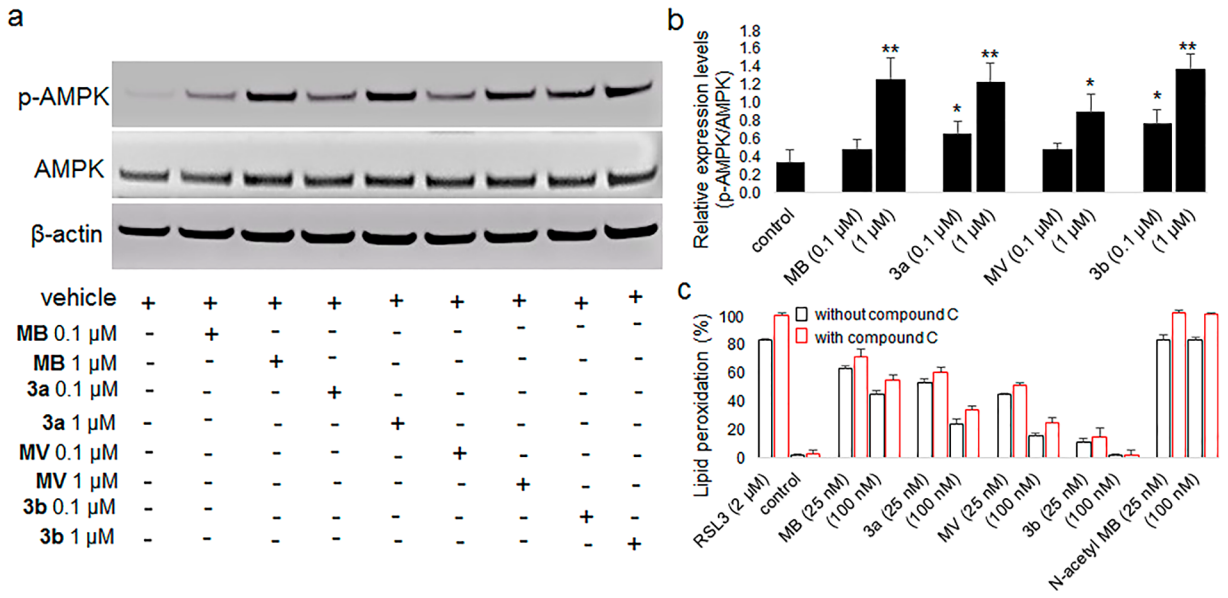

Figure 6. Effect of MB/MV analogues on AMPK and p-AMPK protein expression and their potential as AMPK-mediated inhibitors of ferroptosis. (a) The protein expression levels of AMPK, p-AMPK, and β-actin (loading control) were determined using Western blot analysis in HepG2 cells following treatment with or without MB/MV analogues. (b) Quantification of p-AMPK/AMPK protein expression. Experiments were performed in triplicate and data are expressed as mean ± SEM (*p < 0.05 and **p < 0.01 as compared to control. Statistical analysis was performed using an unpaired, two-tailed t test). (c) Antiferroptotic effects of MB/MV analogues in FRDA lymphocytes against RSL3-induced lipid peroxidation in the presence and absence of AMPK inhibitor compound C (10 μM).

compounds that block ATP production are not likely to find utility as therapeutic agents for Friedreich's ataxia. Thus, the data in Figure 3 support the potential therapeutic utility of analogues such as **1**−**5**.

Mitochondrial inner membrane potential ($\Delta\psi_m$) is another key parameter that is essential for the bioenergetic performance of mitochondria. Accordingly, analogues **1**−**5** were tested for their effects on inner mitochondrial membrane potential in FRDA lymphocytes, using the JC-1 probe as described previously.[33,34] A similar trend was noted for the tested MB/MV analogues (**1**−**5**) on mitochondrial membrane potential, as they had been for total cellular ATP level (Figure 4). As demonstrated in Figure 4, MB and MB analogues with short to medium length side chains (8−12 carbon atoms) exhibited depolarization of $\Delta\psi_m$ at 2.5 μM concentration (Figure 4) while **5a** and **5b** having 16-carbon side chains exhibited no effect at 2.5 μM concentration.

MB exhibits a hormetic dose−response, with opposite effects at low and high doses; this has been attributed to its unique auto-oxidizing properties.[39] In this regard, MB and MB analogues were tested for their cytotoxicity in FRDA cells grown in glucose-free medium containing galactose. Under these nutrient-sensitized conditions, cells rely largely on OXPHOS to produce their ATP and become more sensitive to mitochondrial respiratory chain inhibitors than cells grown in a normal glucose medium.[40] Measurement of cytotoxicity was carried out as described previously.[34] Methylene blue and MB analogues **1a**−**4a**, having 8−12 carbon atom alkyl side chains, exhibited significant cytotoxicity at 2.5 μM concentration (Figure 5). The hydrophilic properties of MB suggest poor cell incorporation and/or their facile autoxidation in the cytosol. More hydrophobic methylene blue analogue **5a** having a 16-carbon side chain lacked cytotoxicity at 0.25 or 2.5 μM concentrations. MV itself was less cytotoxic than methylene blue. Methylene violet and MV analogues **1b**−**3b**, having 8−10 carbon atom alkyl side chains, exhibited some cytotoxicity at 2.5 μM concentration. The modified methylene violet analogues with longer alkyl side chains (**4b**−**5b**) were not cytotoxic under any tested condition. From the results, it is evident that cytotoxicity decreased with increasing lipophilicity. MV and its analogues **1b**−**4b** were less cytotoxic than the corresponding MB analogues. Thus, the experiments in Figures 3, 4, and 5 suggest that the lipophilic analogues of MB and MV studied here have therapeutic potential no less than that of the clinical agent methylene blue.

Recently, Pratt and his co-workers have studied both phenoxazines and phenoxazine-*N*-oxyl as radical trapping antioxidants.[41,42] While neither the substitution patterns of these compounds nor the experimental methods used to measure their activities allow direct comparison with the compounds studied here, both were potent inhibitors of RSL3-induced ferroptosis in mouse embryonic fibroblasts, and both exhibited better potency under the conditions employed than Fer-1 and Lip-1. These observations reinforce the results obtained here and suggest new alternatives to the structures studied in the present report.

MB has been shown to utilize multiple molecular targets and to have beneficial effects clinically.[28−30] Recent studies indicated that MB regulates the energy-sensing AMP-activated protein kinase (AMPK).[43,44] The energy metabolism of the AMPK signaling pathway is also known to impact ferroptosis regulation.[43,44] Some groups studying ferroptosis have found interesting but incompletely understood effects on the regulatory function of AMPK. Song et al. reported that AMPK-mediated BECN1 phosphorylation promotes ferroptosis.[45] In comparison, Lee et al. reported that energy stress activates AMPK that partly suppresses ferroptosis through effects on lipid metabolism.[46] To assess whether AMPK activation by MB/MV analogues is involved in their antiferroptotic activity, we first evaluated the effect of MB,

https://dx.doi.org/10.1021/acsmedchemlett.0c00293
ACS Med. Chem. Lett. XXXX, XXX, XXX−XXX

MV, and analogues **3a** and **3b** on phosphorylated and nonphosphorylated AMPK expression in HepG2 cultured cells. We found that MB, MV, **3a**, and **3b** were able to induce a significant increase in the p-AMPK/AMPK ratio, but only when assayed at higher concentrations than those at which they inhibited ferroptosis. (Figures 6a and b). We next sought to clarify whether inhibition of ferroptosis was due to their radical trapping antioxidant activity or to their ability to stimulate phosphorylation of AMPK or both. We performed a further experiment for these compounds in FRDA lymphocytes involving RSL3-induced lipid peroxidation in the presence and absence of compound C (6-[4-(2-piperidin-1-yl-ethoxy)phenyl]-3-pyridin-4-yl-pyrazolo[1,5-*a*]pyrimidine), a pan inhibitor of AMPK phosphorylation. Figure 6c shows no significant difference in the antiferroptotic activity of the tested compounds in the presence or absence of compound C against RSL3-induced lipid peroxidation at the tested concentrations. The lipid peroxyl radical is a key molecule during the onset of ferroptosis and the treatment with radical scavengers specific for lipid peroxyl radicals represents a promising pharmacologic approach to prevent ferroptosis. Phenothiazines were previously reported to show lipid peroxidation-preventing effects of ferroptosis that were considered to be due to their antioxidant functions.[47−49] Again, when MB was acetylated to eliminate its redox activity, it completely lost its ability to suppress lipid peroxidation despite glutathione depletion in RSL3-treated FRDA lymphocytes (Figure 6c, Table 1). These findings support the interpretation that the MB/MV analogues function primarily as lipid peroxyl radical scavengers, contributing to the prevention of ferroptosis primarily by suppressing lipid peroxidation.

In summary, given the favorable radical trapping antioxidant activity of the MB/MV derivatives relative to Fer-1 and Lip-1, the antiferroptotic activity of lipophilic MB/MV analogues was investigated, as were other properties of the molecules essential to their therapeutic utility, such as their effects on ATP production. Ferroptosis was induced in cultured FRDA cells by GPX4 inhibition with (1*S*,3*R*)-RSL3 or by the cystine/glutamate antiporter (system x_c^- inhibitor erastin). The lipophilic MV analogues were similar to, or had better potency than, ferrostatin-1 and liproxstatin-1. Clearly, there is an optimal side chain length for the MB/MV analogues. In summary, we have identified potent new ferroptosis inhibitors having structures distinct from those of ferrostatin and liproxstatin. These may enable the identification and development of improved ferroptosis inhibitors useful for the therapy of several diseases. While not addressed in the current study, it will certainly be necessary to define the nature of the cellular uptake and distribution of new MB/MV derivatives, as well as the critical cellular loci responsible for the effect(s) of such compounds.

■ ASSOCIATED CONTENT

Supporting Information

The Supporting Information is available free of charge at https://pubs.acs.org/doi/10.1021/acsmedchemlett.0c00293.

Details of the synthesis and characterization of new compounds, as well as bioassay protocols (PDF)

NMR spectra of compounds **10**−**15**, **1a**−**4a**, and **1b**−**4b** (PDF)

■ AUTHOR INFORMATION

Corresponding Authors

Omar M. Khdour − *Biodesign Center for BioEnergetics, Arizona State University, Tempe, Arizona 85287, United States*; Email: khdour@asu.edu

Sidney M. Hecht − *Biodesign Center for BioEnergetics and School of Molecular Sciences, Arizona State University, Tempe, Arizona 85287, United States*; orcid.org/0000-0002-5429-2462; Email: sid.hecht@asu.edu

Authors

Jun Liu − *Biodesign Center for BioEnergetics, Arizona State University, Tempe, Arizona 85287, United States*

Indrajit Bandyopadhyay − *Biodesign Center for BioEnergetics and School of Molecular Sciences, Arizona State University, Tempe, Arizona 85287, United States*

Lei Zheng − *Biodesign Center for BioEnergetics, Arizona State University, Tempe, Arizona 85287, United States*

Complete contact information is available at: https://pubs.acs.org/10.1021/acsmedchemlett.0c00293

Funding

This work was supported in part by a research grant from the Friedreich's Ataxia Research Alliance (FARA).

Notes

The authors declare no competing financial interest.

■ ABBREVIATIONS

FRDA, Friedreich's Ataxia; MB, methylene blue; MV, methylene violet; FXN, frataxin; ROS, reactive oxygen species; GPX4, glutathione peroxidase 4; GSH, glutathione; FSP-1, ferroptosis-suppressor-protein 1; Fer-1, ferrostatin; Lip-1, liproxstatin-1; RSL-3, RAS-selective lethal 3; α-TOH, α-tocopherol; OXPHOS, oxidative phosphorylation; AMPK, AMP-activated protein kinase

■ REFERENCES

(1) Campuzano, V.; Montermini, L.; Moltò, M. D.; Pianese, L.; Cossee, M.; Cavalcanti, F.; Monros, E.; Rodius, F.; Duclos, F.; Monticelli, A.; Zara, F.; Cañizares, J.; Koutnikova, H.; Bidichandani, S. I.; Gellera, C.; Brice, A.; Trouillas, P.; De Michele, G.; Filla, A.; De Frutos, R.; Palau, F.; Patel, P. I.; Di Donato, S.; Mandel, J. L.; Cocozza, S.; Koenig, M.; Pandolfo, M. Friedreich's Ataxia: Autosomal Recessive Disease Caused by an Intronic GAA Triplet Repeat Expansion. *Science* **1996**, *271*, 1423−1427.

(2) Bidichandani, S. I.; Ashizawa, T.; Patel, P. I. The GAA Triplet-Repeat Expansion in Friedreich Ataxia Interferes with Transcription and May be Associated with an Unusual DNA Structure. *Am. J. Hum. Genet.* **1998**, *62*, 111−121.

(3) Gerber, J.; Mühlenhoff, U.; Lill, R. An Interaction between Frataxin and Isu1/Nfs1 that is Crucial for Fe/S Cluster Synthesis on Isu1. *EMBO Rep.* **2003**, *4*, 906−911.

(4) Schmucker, S.; Martelli, A.; Colin, F.; Page, A.; Wattenhofer-Donzé, M.; Reutenauer, L.; Puccio, H. Mammalian Frataxin: an Essential Function for Cellular Viability through an Interaction with a Preformed ISCU/NFS1/ISD11 Iron-Sulfur Assembly Complex. *PLoS One* **2011**, *6*, e16199.

(5) Bridwell-Rabb, J.; Fox, N. G.; Tsai, C. L.; Winn, A. M.; Barondeau, D. P. Human Frataxin Activates Fe−S Cluster Biosynthesis by Facilitating Sulfur Transfer Chemistry. *Biochemistry* **2014**, *53*, 4904−4913.

(6) Delatycki, M. B.; Camakaris, J.; Brooks, H.; Evans-Whipp, T.; Thorburn, D. R.; Williamson, R.; Forrest, S. M. Direct Evidence that Mitochondrial Iron Accumulation Occurs in Friedreich Ataxia. *Ann. Neurol.* **1999**, *45*, 673−675.

(7) Richardson, D. R.; Huang, M. L.; Whitnall, M.; Becker, E. M.; Ponka, P.; Suryo Rahmanto, Y. The Ins and Outs of Mitochondrial Iron-Loading: the Metabolic Defect in Friedreich's Ataxia. *J. Mol. Med. (Heidelberg, Ger.)* **2010**, *88*, 323−329.
(8) Armstrong, J. S.; Khdour, O.; Hecht, S. M. Does Oxidative Stress Contribute to the Pathology of Friedreich's Ataxia? A Radical Question. *FASEB J.* **2010**, *24*, 2152−2163.
(9) Cotticelli, M. G.; Crabbe, A. M.; Wilson, R. B.; Shchepinov, M. S. Insights into the Role of Oxidative Stress in the Pathology of Friedreich Ataxia Using Peroxidation Resistant Polyunsaturated Fatty Acids. *Redox Biol.* **2013**, *1*, 398−404.
(10) Cotticelli, M. G.; Xia, S.; Lin, D.; Lee, T.; Lin, D.; Terrab, L.; Wipf, P.; Huryn, D.; Wilson, R. B. Ferroptosis as a Novel Therapeutic Target for Friedreich's Ataxia. *J. Pharmacol. Exp. Ther.* **2019**, *369*, 47−54.
(11) Abeti, R.; Parkinson, M. H.; Hargreaves, I. P.; Angelova, P. R.; Sandi, C.; Pook, M. A.; Giunti, P.; Abramov, A. Y. Mitochondrial Energy Imbalance and Lipid Peroxidation Cause Cell Death in Friedreich's Ataxia. *Cell Death Dis.* **2016**, *7*, e2237.
(12) Abeti, R.; Uzun, E.; Renganathan, I.; Honda, T.; Pook, M. A.; Giunti, P. Targeting Lipid Peroxidation and Mitochondrial Imbalance in Friedreich's Ataxia. *Pharmacol. Res.* **2015**, *99*, 344−350.
(13) Dixon, S. J.; Lemberg, K. M.; Lamprecht, M. R.; Skouta, R.; Zaitsev, E. M.; Gleason, C. E.; Patel, D. N.; Bauer, A. J.; Cantley, A. M.; Yang, W. S.; Morrison, B., 3rd.; Stockwell, B. R. Ferroptosis: an Iron-Dependent Form of Nonapoptotic Cell Death. *Cell* **2012**, *149*, 1060−1072.
(14) Latunde-Dada, G. O. Ferroptosis: Role of Lipid Peroxidation, Iron and Ferritinophagy. *Biochim. Biophys. Acta, Gen. Subj.* **2017**, *1861*, 1893−1900.
(15) Cao, J. Y.; Dixon, S. J. Mechanisms of Ferroptosis. *Cell. Mol. Life Sci.* **2016**, *73*, 2195−2209.
(16) Xie, Y.; Hou, W.; Song, X.; Yu, Y.; Huang, J.; Sun, X.; Kang, R.; Tang, D. Ferroptosis: Process and Function. *Cell Death Differ.* **2016**, *23*, 369−379.
(17) Yang, W. S.; Stockwell, B. R. Synthetic Lethal Screening Identifies Compounds Activating Iron-Dependent, Nonapoptotic Cell Death in Oncogenic-RAS-Harboring Cancer Cells. *Chem. Biol.* **2008**, *15*, 234−245.
(18) Liang, H.; Yoo, S. E.; Na, R.; Walter, C. A.; Richardson, A.; Ran, Q. Short Form Glutathione Peroxidase 4 is the Essential Isoform Required for Survival and Somatic Mitochondrial Functions. *J. Biol. Chem.* **2009**, *284*, 30836−30844.
(19) Yang, W. S.; SriRamaratnam, R.; Welsch, M. E.; Shimada, K.; Skouta, R.; Viswanathan, V. S.; Cheah, J. H.; Clemons, P. A.; Shamji, A. F.; Clish, C. B.; Brown, L. M.; Girotti, A. W.; Cornish, V. W.; Schreiber, S. L.; Stockwell, B. R. Regulation of Ferroptotic Cancer Cell Death by GPX4. *Cell* **2014**, *156*, 317−331.
(20) Yant, L. J.; Ran, Q.; Rao, L.; Van Remmen, H.; Shibatani, T.; Belter, J. G.; Motta, L.; Richardson, A.; Prolla, T. A. The Selenoprotein GPX4 is Essential for Mouse Development and Protects from Radiation and Oxidative Damage Insults. *Free Radical Biol. Med.* **2003**, *34*, 496−502.
(21) Dolma, S.; Lessnick, S. L.; Hahn, W. C.; Stockwell, B. R. Identification of Genotype-Selective Antitumor Agents Using Synthetic Lethal Chemical Screening in Engineered Human Tumor Cells. *Cancer Cell* **2003**, *3*, 285−296.
(22) Meister, A. Selective Modification of Glutathione Metabolism. *Science* **1983**, *220*, 472−477.
(23) Bannai, S.; Tateishi, N. Role of Membrane Transport in Metabolism and Function of Glutathione in Mammals. *J. Membr. Biol.* **1986**, *89*, 1−8.
(24) Dixon, S. J.; Patel, D. N.; Welsch, M.; Skouta, R.; Lee, E. D.; Hayano, M.; Thomas, A. G.; Gleason, C. E.; Tatonetti, N. P.; Slusher, B. S.; Stockwell, B. R. Pharmacological Inhibition of Cystine-Glutamate Exchange Induces Endoplasmic Reticulum Stress and Ferroptosis. *eLife* **2014**, *3*, No. e02523.
(25) Doll, S.; Freitas, F. P.; Shah, R.; Aldrovandi, M.; da Silva, M. C.; Ingold, I.; Grocin, A. G. FSP1 is a Glutathione-Independent Ferroptosis Suppressor. *Nature* **2019**, *575*, 693−698.
(26) Bersuker, K.; Hendricks, J.; Li, Z.; Magtanong, L.; Ford, B.; Tang, P. H.; Roberts, M. A.; Tong, B.; Maimone, T. J.; Zoncu, R.; Bassik, M. C.; Nomura, D. K.; Dixon, S. J.; Olzmann, J. A. The CoQ Oxidoreductase FSP1 Acts Parallel to GPX4 to Inhibit Ferroptosis. *Nature* **2019**, *575*, 688−692.
(27) Han, C.; Liu, Y.; Dai, R.; Ismail, N.; Su, W.; Li, B. Ferroptosis and Its Potential Role in Human Diseases. *Front. Pharmacol.* **2020**, *11*, 239.
(28) Jaszczyszyn, A.; Gąsiorowski, K.; Swiątek, P.; Malinka, W.; Cieślik-Boczula, K.; Petrus, J.; Czarnik-Matusewicz, B. Chemical Structure of Phenothiazines and Their Biological Activity. *Pharmacol. Rep.* **2012**, *64*, 16−23.
(29) Atamna, H.; Nguyen, A.; Schultz, C.; Boyle, K.; Newberry, J.; Kato, H.; Ames, B. N. Methylene Blue Delays Cellular Senescence and Enhances Key Mitochondrial Biochemical Pathways. *FASEB J.* **2008**, *22*, 703−712.
(30) Wen, Y.; Li, W.; Poteet, E. C.; Xie, L.; Tan, C.; Yan, L. J.; Ju, X.; Liu, R.; Qian, H.; Marvin, M. A.; Goldberg, M. S.; She, H.; Mao, Z.; Simpkins, J. W.; Yang, S. H. Alternative Mitochondrial Electron Transfer as a Novel Strategy for Neuroprotection. *J. Biol. Chem.* **2011**, *286*, 16504−16515.
(31) Poteet, E.; Winters, A.; Yan, L.-J.; Shufelt, K.; Green, K. N.; Simpkins, J. W.; Wen, Y.; Yang, S. H. Neuroprotective Actions of Methylene Blue and its Derivatives. *PLoS One* **2012**, *7*, e48279.
(32) Roy Chowdhury, S.; Khdour, O. M.; Bandyopadhyay, I.; Hecht, S. M. Lipophilic Methylene Violet Analogues as Modulators of Mitochondrial Function and Dysfunction. *Bioorg. Med. Chem.* **2017**, *25*, 5537−5547.
(33) Khdour, O. M.; Bandyopadhyay, I.; Chowdhury, S. R.; Visavadiya, N. P.; Hecht, S. M. Lipophilic Methylene Blue Analogues Enhance Mitochondrial Function and Increase Frataxin Levels in a Cellular Model of Friedreich's Ataxia. *Bioorg. Med. Chem.* **2018**, *26*, 3359−3369.
(34) Khdour, O. M.; Bandyopadhyay, I.; Visavadiya, N. P.; Roy Chowdhury, S.; Hecht, S. M. Phenothiazine Antioxidants Increase Mitochondrial Biogenesis and Frataxin Levels in Friedreich's Ataxia Cells. *MedChemComm* **2018**, *9*, 1491−1501.
(35) Yang, W. S.; Stockwell, B. R. Ferroptosis: Death by Lipid Peroxidation. *Trends Cell Biol.* **2016**, *26*, 165−176.
(36) Fash, D. M.; Khdour, O. M.; Sahdeo, S. J.; Goldschmidt, R.; Jaruvangsanti, J.; Dey, S.; Arce, P. M.; Collin, V. C.; Cortopassi, G. A.; Hecht, S. M. Effects of Alkyl Side Chain Modification of Coenzyme Q_{10} on Mitochondrial Respiratory Chain Function and Cytoprotection. *Bioorg. Med. Chem.* **2013**, *21*, 2346−2354.
(37) Martinez, A. M.; Kim, A.; Yang, W. S. Detection of Ferroptosis by BODIPY 581/591 C11. In *Immune Mediators in Cancer*; Vancurova, I., Zhu, Y., Eds.; Methods in Molecular Biology; Humana: New York, NY, 2020; Vol. *2108*, pp 125−130.
(38) Tretter, L.; Horvath, G.; Holgyesi, A.; Essek, F.; Adam-Vizi, V. Enhanced Hydrogen Peroxide Generation Accompanies the Beneficial Bioenergetic Effects of Methylene Blue in Isolated Brain Mitochondria. *Free Radical Biol. Med.* **2014**, *77*, 317−330.
(39) Rojas, J. C.; Bruchey, A. K.; Gonzalez-Lima, F. Neurometabolic Mechanisms for Memory Enhancement and Neuroprotection of Methylene Blue. *Prog. Neurobiol.* **2012**, *96*, 32−45.
(40) Aguer, C.; Gambarotta, D.; Mailloux, R. J.; Moffat, C.; Dent, R.; McPherson, R.; Harper, M. E. Galactose Enhances Oxidative Metabolism and Reveals Mitochondrial Dysfunction in Human Primary Muscle Cells. *PLoS One* **2011**, *6*, e28536.
(41) Farmer, L. A.; Haidasz, E. A.; Griesser, M.; Pratt, D. A. Phenoxazine: A Privileged Scaffold for Radical-Trapping Antioxidants. *J. Org. Chem.* **2017**, *82*, 10523−10536.
(42) Griesser, M.; Shah, R.; Van Kessel, A. T.; Zilka, O.; Haidasz, E. A.; Pratt, D. A. The Catalytic Reaction of Nitroxides with Peroxyl Radicals and Its Relevance to Their Cytoprotective Properties. *J. Am. Chem. Soc.* **2018**, *140*, 3798−3808.

https://dx.doi.org/10.1021/acsmedchemlett.0c00293
ACS Med. Chem. Lett. XXXX, XXX, XXX−XXX

(43) Atamna, H.; Atamna, W.; Al-Eyd, G.; Shanower, G.; Dhahbi, J. M. Combined Activation of the Energy and Cellular-Defense Pathways May Explain the Potent Anti-senescence Activity of Methylene Blue. *Redox Biol.* **2015**, *6*, 426−435.
(44) Xie, L.; Li, W.; Winters, A.; Yuan, F.; Jin, K.; Yang, S. Methylene Blue Induces Macroautophagy through 5′ Adenosine Monophosphate-Activated Protein Kinase Pathway to Protect Neurons from Serum Deprivation. *Front. Cell. Neurosci.* **2013**, *7*, 56.
(45) Song, X.; Zhu, S.; Chen, P.; Hou, W.; Wen, Q.; Liu, J.; Xie, Y.; Liu, J.; Klionsky, D. J.; Kroemer, G.; Lotze, M. T.; Zeh, H. J.; Kang, R.; Tang, D. AMPK-mediated BECN1 Phosphorylation Promotes Ferroptosis by Directly Blocking System xc(−) Activity. *Curr. Biol.* **2018**, *28*, 2388−2399 (e2385).
(46) Lee, H.; Zandkarimi, F.; Zhang, Y.; Meena, J. K.; Kim, J.; Zhuang, L.; Tyagi, S.; Ma, L.; Westbrook, T. F.; Steinberg, G. R.; Nakada, D.; Stockwell, B. R.; Gan, B. Energy-Stress-Mediated AMPK Activation Inhibits Ferroptosis. *Nat. Cell Biol.* **2020**, *22*, 225−234.
(47) Mishima, E.; Sato, E.; Ito, J.; Yamada, K. I.; Suzuki, C.; Oikawa, Y.; Matsuhashi, T.; Kikuchi, K.; Toyohara, T.; Suzuki, T.; Ito, S.; Nakagawa, K.; Abe, T. Drugs Repurposed as Antiferroptosis Agents Suppress Organ Damage, Including AKI, by Functioning as Lipid Peroxyl Radical Scavengers. *J. Am. Soc. Nephrol.* **2020**, *31*, 280−296.
(48) Shah, R.; Margison, K.; Pratt, D. A. The Potency of Diarylamine Radical-Trapping Antioxidants as Inhibitors of Ferroptosis Underscores the Role of Autoxidation in the Mechanism of Cell Death. *ACS Chem. Biol.* **2017**, *12*, 2538−2545.
(49) Keynes, R.; Karchevskaya, A.; Riddall, D.; Griffiths, C. H.; Bellamy, T. C.; Chan, A. W. E.; Selwood, D. L.; Garthwaite, J. N10-Carbonyl-Substituted Phenothiazines Inhibiting Lipid Peroxidation and Associated Nitric Oxide Consumption Powerfully Protect Brain Tissue Against Oxidative Stress. *Chem. Biol. Drug Des.* **2019**, *94*, 1680−1693.

https://dx.doi.org/10.1021/acsmedchemlett.0c00293
ACS Med. Chem. Lett. XXXX, XXX, XXX−XXX